Multivariable control and online state estimation of an FCC unit

Alexandre Teplaira Boum, Mohamed Abderrazak Latifi, Jean-Pierre Corriou

Jestr

Journal of Engineering Science and Technology Review 8 (3) (2015) 158-168

JOURNAL OF
Engineering Science and Technology Review

Research Article

www.jestr.org

Multivariable Control and Online State Estimation of an FCC Unit

A. T. Boum[1], A. Latifi[2] and J. P. Corriou[2]

[1]*Universite de Douala, ENSET B.P 1872 Douala, Cameroun*
[2]*Universite de Lorraine, LRGP, UMR 3349, Nancy, F-54001, France*

Received 7 July 2015; Accepted 20 October 2015

Abstract

The purpose of this paper is to realize multivariable control , tuning and online state estimation of some parameters of the FCC unit . We implemented two control structures with the manipulated variables being the air inlet flow rate in the regenerator, the regenerated catalyst flow rate and the feed flow rate and, the controlled variable being the temperatures in the riser and in the densed bed of the regenerator. A novel four transfer function is built and used for controllability studies. Hard constraints are imposed with respect to the manipulated variables. Simulation results show that the configuration made of two inputs and two outputs is more easy to tune for control purposes. Althought there are important dynamic interactions between the components of the FCC and important nonlinearities, linear model predictive control is able to maintain a smooth multivariable control of the plant, while taking into account the different constraints. Tuning strategy is implemented to improve the tracking of the set point. Online state estimation is carried out with the use of the extended Kalman filter. The estimation gives results that can be used for monitoring purposes even in the presence of model mismatch.

Keywords: Multivariable; Identification; Model predictive control; Extended kalman filter

1 Introduction

Fluid caalytic cracking (FCC) is of essential economic importance in a modern refinery. This is due to the fact that fluid catalytic cracking is used to crack heavy atmospheric residues and vacuum distillate into lighter molecules that can yield more valuable products. The FCC unit is a complex process [19] . Its complexity is due to the complex chemical reactions and dynamic interactions that take place in its main units, namely riser, separator and regenerator. The complex nature of this process make it a challenge to scientists and engineers in the field of control. In order to maximize the gains, this plant must be operated close to constraints [19] . Model predictive control (MPC) is used due to its capacity to take into account hard and soft constraints with respect to the manipulated variables, their moves and the controlled variables even with a multivriable process.

In this work, linear Model Predictive Control (MPC) of the FCC with two control structures, tuning and online states estimation with the use of extended Kalman filter are addressed. The organization of this paper is as follows, Section 2 is related to the process description. Section 3 describes the model of FCC. Section 4 deals with model predictive control principles. Section 5 deals with model identification. Section 6 deals with controlability of the FCC. Section 7 deals with the control of the FCC unit with the discussions of the simulation results. Section 8 deals with the tuning of MPC parameters. Section 9 deals with online state estimation. Finally, the conclusions of the paper are presented in Section 10.

2 Description of a modern FCC process

An FCC process consists of three main units (Figure 1). The cracking reactions of the hydrocarbon feed take place in the riser while the catalyst is reactivated in the regenerator by combustion of the coke deposited on the catalyst in the riser reactor.

The temperature of the preheated feed is in the range of 450-600K. This feed is injected in the bottom of the riser with a small quantity of vapor. At the contact of the hot catalyst from the regenerator in the range of 900-1100K, the feed is vaporised . The resulting hydrocarbon vapors undergo an endothermic reaction while rising to the top of the riser. This rising is due to a great pressure at the bottom of the riser and the low density of the mixing of catalyst and vapors. The residence time of the catalyst and the hydrocarbon vapors (supposing that the solid catalyst and the hydrocarbons have the same residence time) in the riser is a few seconds. The temperature at the top of the riser is between 750 and 820K. The disengagement part of the reactor is used to separate the catalyst particles from the vapors with the use of cyclones. The spent catalyst is separated from the vapors and flows in the extraction part where the remaining hydrocarbons on its surface are removed by injection of stripping steam. The catalyst flows through a transport line to the regenerator.

The air entering the regenerator is used to burn the

* E-mail address: boumat2002@yahoo.fr
ISSN: 1791-2377

deposited coke on the catalyst. This partial or total exothermic combustion reaction reactivates the catalyst and maintains the bed temperature between 950-980K for future gasoil cracking. The regenerated catalyst flows in the riser through another circuit. The heat from the regenerator is used to compensate the endothermic reactions in the riser.

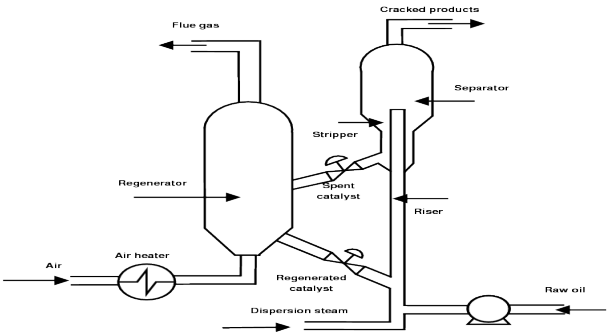

Fig. 1. Schematic diagram of FCC unit

3 Mathematical model of the FCC

There are many models found in the litterature with more or less details. Some are for design, optimization or control purposes. The FCC model used is mainly destined for control purposes [1] and is adapted from [17] with some modifications by [3, 16]. This model describes the main dynamical aspects of an FCC unit and is adequate for predictive control because the main objectives of an FCC model are a description of the regenerator dynamics and a description of gasoline yield [2, 19]. Some important equations are presented in this work but a more detailed description of this model is found in [4, 5, 15].

Energy balance in the riser

$$\frac{dT_{ris}}{dz} = \frac{\Delta H_{crack} F_{feed}}{(F_{regcat} C_{pcat} + F_{feed} C_{po} + \lambda F_{feed} C_{psteam})} \frac{dy_{go}}{dz} \tag{1}$$

Energy balance in the separator

$$\frac{dT_{sep}}{dt} = \frac{C_{p,cat} F_{cat,spent} (T_{ris,1} - T_{sep})}{m_{cat,sep} C_{p,cat}} \tag{2}$$

where $T_{ris,1}$ is the temperature at the riser top.

Mass Balance of coke on the catalyst

$$\frac{dC_{coke,reg}}{dt} = \frac{(F_{cat,spent} C_{coke,sep} - F_{cat,reg} C_{coke,reg}) - R_{cb}}{m_{cat,reg}} \tag{3}$$

$F_{cat,reg}$ is the flow rate of the regenerated catalyst ($kg.s^{-1}$), $C_{coke,reg}$ mass fraction of coke in the regenerator, $m_{cat,reg}$ hold up of catalyst in the regenerator (kg), R_{cb} kinetic of coke combustion (s).

Energy balance in the regenerator

$$\frac{dT_{reg}}{dt} = \frac{1}{(m_{catreg} C_{pcat})} [(T_{sep} F_{spentcat} C_{pcat} + T_{air} F_{masregair} C_{pair} - T_{reg} (F_{regcat} C_{pcat} + F_{masregair} C_{pair}) - \Delta H_{cb} \frac{R_{cb}}{M_{wcoke}}] \tag{4}$$

coke combustion kinetic is given by

$$R_{cb} = k_{cb} \exp(-\frac{E_{acb}}{RT_{reg}}) x_{O2} C_{cokereg} m_{catreg} \tag{5}$$

4 Model predictive control

Model Predictive Control (MPC) is not a tool in itself but, represents a class of algorithms that use a process model to maintain the controlled variables of a given process close as possible to the set point while taking into account the different constraints . MPC was first implemented by [20], then Dynamic Matrix Control (DMC) was introduced [7, 9]. Nowadays, there are many algorithms for model predictive implementation ranging from linear one to nonlinear [10, 13]. In the present work, linear model predictive control is used and step responses are also used for system identification, the corresponding algorithms are briefly described. DMC [9] minimizes a quadratic criterion without taking into account the constraints so that an analytical solution can be found for the control vector. Quadratic dynamic matrix control (QDMC) [11, 12] minimizes a criterion in while taking into account constraints. In this study, quadratic dynamic matrix control was used with constraints imposed on the manipulated variables and their variations. The code used has been developed in Fortran90.

5 Open loop identification

5.1 Simulation parameters

The parameters that are used for FCC control are found in Tables 1 and 2. Table 1 gives the stationary values obtained by integration of the dynamic equations of the nonlinear model until a steady state is found for given values of manipulated inputs.

Table 1. Steady state values of important variable for the FCC

Symbole	Signification	Value
C_{Ccreg}	Coke concentration in the regenerator (kg/kg)	0.0038
C_{Ccsep}	Coke concentration in the riser at Z-1 (kg/kg)	0.0104
$T_{ris}(0)$	Temperature in the riser at Z=0 (K)	805
T_{sep}	Temperature in the riser at Z=1 (K)	780.62
T_{reg}	Temperature in the dense bed of the regenerator (K)	971.92
x_{o_2}	Molar fraction of oxygen in the regenerator	0.0047
y_{g0}	Mass fraction of oil in the riser at Z=1	0.4825

y_g	Mass fraction of oil in the riser at Z=1	0.3680

Table 2. FCC data used in the simulation

Symbol	Meaning	Value
$C_{p,air}$	heat capacity of air (J.kg^{-1}.K^{-1})	1074
$C_{p,o}$	heat capacity of oil (J.kg^{-1}.K^{-1})	2671
$C_{p,steam}$	heat capacity of steam (J.kg^{-1}.K^{-1})	1900
E_{acf}	activation energy for coke formation (J.mol^{-1})	2089.5
E_{af}	activation energy for cracking of gas oil (feed) (J.mol^{-1})	101.510^3
E_{ag}	activation energy for cracking of gasoline (J.mol^{-1})	112.610^3
$F_{air,reg}$	mass flow rate of air to regenerator (kg.s^{-1})	25.378
$F_{cat,reg}$	mass flow rate of catalyst (kg.s^{-1})	294
F_{feed}	mass feed flow rate (kg.s^{-1})	40.63
$m_{air,reg}$	holdup of air in the regenerator (mol)	20000
$m_{cat,reg}$	holdup of catalyst in regenerator (kg)	175738
$m_{cat,sep}$	holdup of catalyst in separator (kg)	17500
$M_{w,coke}$	molar weight of coke (kg.mol^{-1})	14.10^{-3}
n_{CH}	number of moles of hydrogen per mole of carbon in the coke	2
T_{air}	temperaure of air to regenerator (K)	360
T_{boil}	boiling temperature of the feed (K)	700
t_c	residence time in the riser (s)	9.6
T_{feed}	feed temperature (K)	434.63
ΔH_{vap}	heat of feed vaporization (J.kg^{-1})	1.5610^5
ΔH_{crack}	heat of cracking (J.kg^{-1})	506.210^3
α_2	fraction of gas oil which cracks to gasoline	0.75

The manipulated variables are the regenerated catalyst flow rate and the flow rate of air to the regenarator; The controlled variables are the temperature at the top of the riser and the temperature in the regenerator dense bed (Table 3).

Table 3. Manipulated variable and controlled variables

2X2 control		
Input 1	Regenerated catalyst	u_1
Input 2	Flow rate of air into the regenerator	u_2
Output 1	Temperature at the top of the riser	y_1
Output 2	Temperature in the regenerator dense bed	y_2

In order to carry out open loop identification of our system, step inputs are applied resulting in the responses of figures 3 and 4 according to (2). From a steady value of the catalyst flow rate equal to 294 kg.s^{-1}, a step of $+5$% is applied, from a steady state value of the flow rate of air equal to 25.378 kg.s^{-1}, a step of $+0.05$% is applied.

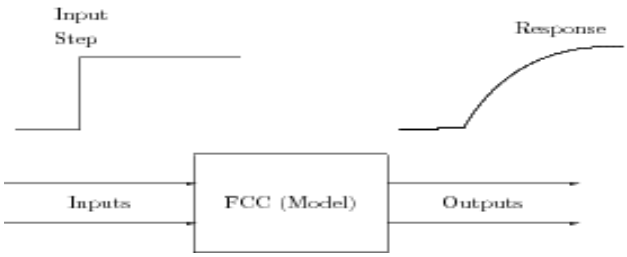

Fig. 2. Identification process

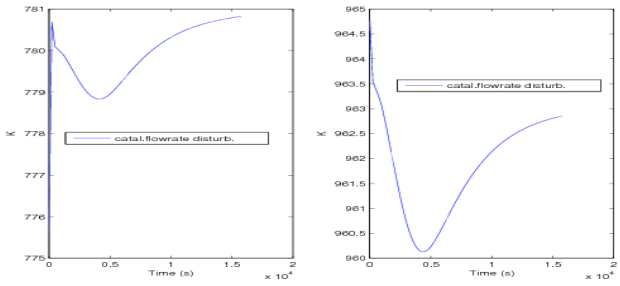

Fig. 3. Open loop response to a flow rate step of catalyst: temperature at the top of the (left), temperature in the regenerator (right)

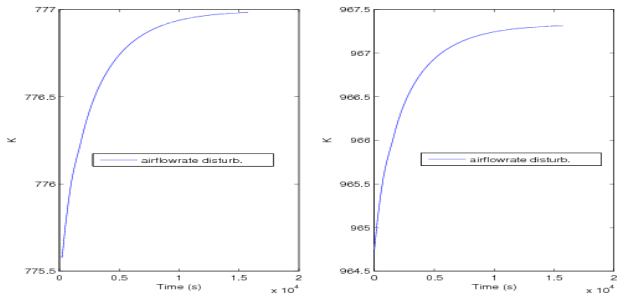

Fig . 4. Open loop response to a flow rate step of air: temperature at the top of the riser (left), temperature in the regenerator (right)

The step responses obtained are presented in Figure 5. For the catalyst flow rate step u_1, the temperature at the riser top y_1 and the temperature in the regenerator y_2 follow an inverse response. In fact, the increase of catalyst flow rate increases abruptly the temperature at the bottom of the riser, hence the one at the top of the riser without dynamic effect; then, the temperature decreases dynamically due to the endothermicity of the cracking reactions and increases slowly due to the exothermicity of the regenerator and its great thermal inertia. At the opposite, for the air flow rate step u_2, the responses are close to first order transfer functions. In fact, the increase of the flow rate of air enhances the exothermic combustion reaction in the regenerator and consequently the temperature of the regenerator according to a first order process. The regenerator temperature is also that of regenerated catalyst which influences the temperature at the bottom of the riser and consequently that of the riser top.

Using a sampling period $T_s = 250$s, the step response coefficients are calculated (Figure 5) which enable us to

build the dynamic matrix A used in DMC and QDMC control algorithms.

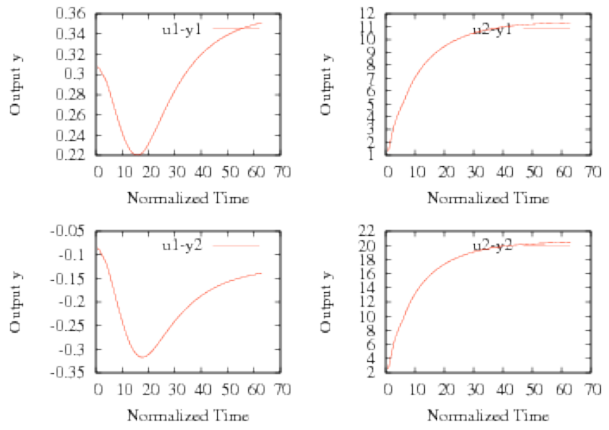

Fig 5. Coefficients of the step response: u_1 flow rate of catalyst, u_2 flow rate of air, y_1 riser temperature, y_2 regenerator temperature

6 Controllability of the FCC

The controllability of the FCC model used have been studied by [16] using the relative gain array [8]. [2] gives the possible combination of manipulated variables and controlled variables for partial and complete combustion mode. As previously mentioned, the controlled variables T_{ris}, T_{reg} and manipulated variables F_{air}, F_{cat} are chosen.

The choice of the structure of the control variables is also important [15] and the relative gain array is a useful tool to examine the coupling of the manipulated and controlled variables in a multivariable process. This tool was proposed by [6]. It enables us to choose the best coupling between inputs and ouputs. [18] used it for the design of a regulator for the FCC. For controller that are not multivariable like the PID, it permits to be sure of the controllability of the system with the selected input-output structure.

According to Figure 5, the transfer functions corresponding to the step responses have been identified with the following model coupling an algebraic response and an inverse response for the couples $(u_1 - y_1)$ and $(u_1 - y_2)$ as:

$$G_{1i}(s) = a_i + \frac{K_{2i}}{\tau_{2i}s+1} - \frac{K_{1i}}{\tau_{1i}s+1} \tag{6}$$

and first order transfer functions for the couples $(u_2 - y_1)$ and $(u_2 - y_2)$ as:

$$G_{2i}(s) = \frac{K'_{2i}}{\tau'_{2i}s+1} \tag{7}$$

According to the previous transfer functions, the time responses to a unity input step have been calculated respectively as:

$$\delta y_{1i}(t) = a_i H(t) + K_{2i}\left(1-\exp\left(-\frac{t}{\tau_{2i}}\right)\right) - K_{1i}\left(1-\exp\left(-\frac{t}{\tau_{1i}}\right)\right) \tag{8}$$

and:

$$\delta y_{2i}(t) = K'_{2i}\left(1-\exp\left(-\frac{t}{\tau'_{2i}}\right)\right) \tag{9}$$

where $H(t)$ is the Heaviside function.

Table 4. Identified continuous transfer functions

Symbol	Couple	Transfert function
G_{11}	$(u_1 - y_1)$	$0.32 + \frac{5.887}{3010s+1} - \frac{5.847}{2827s+1}$
G_{12}	$(u_1 - y_2)$	$-0.08 + \frac{7.711}{3102s+1} - \frac{7.751}{2884s+1}$
G_{21}	$(u_2 - y_1)$	$\frac{11.039}{2853s+1}$
G_{22}	$(u_2 - y_2)$	$\frac{19.904}{2348s+1}$

The identification has been performed by minimizing a least squares criteria comparing the step responses y_{exp} and the time response of the model y_{mod} to a unity input step:

$$J = \sum_{i=1}^{n} w(i)(y_{exp}(i) - y_{mod}(i))^2 \tag{10}$$

In the case of transfer functions $G_{1i}(s)$, the weight $w(i)$ were equal to 1 when $i \le 15$ and equal to 10 when $i \ge 16$ in order to give more weight to the final form of the shape of the response. For transfer functions $G_{2i}(s)$, the weights $w(i)$ were all equal to 1. For transfer functions (6), knowing the approximate value of the final response, a constraint was imposed:

$$\delta y_{1i}(\infty) = a_i + K_{2i} - K_{1i} \tag{11}$$

with a_i read on the step response. For these transfer functions, three parameters were thus identified. For transfer functions (7), K'_{2i} could have directly determined, but a simple identification with two parameters was carried out. Using the function "fminsearch" of Matlab, the transfer functions parameters have been obtained (Table 4). On the figures 6, the step response and the response of identified model are compared and show a satisfactory agreement for the response with the input u_1 (catalyst flow rate) and a very good agreement for the response with the input u_2 (flow rate of air).

For the response to the input u_1 (flow rate of catalyst), the time constant τ_2 is slightly greater than τ_1. The catalyst residence time in the riser is negligible, the residence time of catalyst in the separator is equal to 59.5s and the residence time of catalyst in the regenerator is equal to 597.7s. Thus, the time constants of the identified transfer functions (Table 4) are about 4 to 5 times the greater residence time.

For the relative gain matrix, the transfer functions

$G_{1i}(s)$ (eq. 6) are approximated as first order transfer functions with gain K_{1i}. The following gains were deduced:

$$K_{11}=0.36,\quad K_{12}=-0.12,\quad K_{21}=11.039,\quad K_{22}=19.904 \tag{12}$$

Hence, the relative gain array matrix RGA can be determined knowing that:

$$\lambda_{11}=\frac{(\partial y_1/\partial u_1)_{u_2}}{(\partial y_1/\partial u_1)_{y_2}}=\frac{1}{1-k} \tag{13}$$

with $$k=\frac{K_{12}K_{21}}{K_{11}K_{22}}=-0.185 \tag{14}$$

The relative gain array matrix (RGA) results as:

$$\Lambda=\begin{bmatrix}\lambda_{11} & \lambda_{12}\\ \lambda_{21} & \lambda_{22}\end{bmatrix}=\begin{bmatrix}0.845 & 0.155\\ 0.155 & 0.845\end{bmatrix} \tag{15}$$

If the matrix Λ were the identity matrix, the system would be perfectly decoupled [8]. In the present case, the element λ_{11} is close to 1. The chosen coupling (y_1 coupled to u_1 and y_2 coupled to u_2, i.e. the temperature at the top of the riser coupled to the flow rate of catalyst and the temperature of the regenerator coupled to the flow rate of air), would allow an efficient control of the FCC with PID controllers.

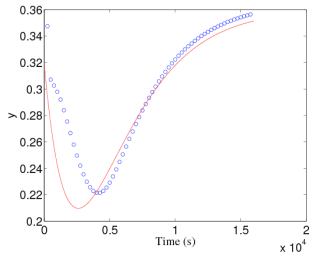

(a) Step response of the system and transfer function u_1-y_1)

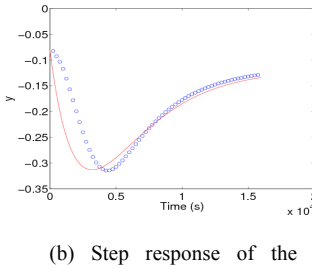

(b) Step response of the system and transfer function u_1-y_2)

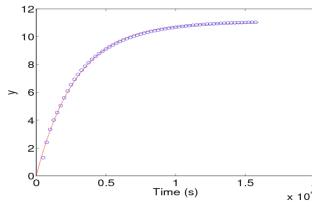

(c) Step response of the system and transfer function u_2-y_1)

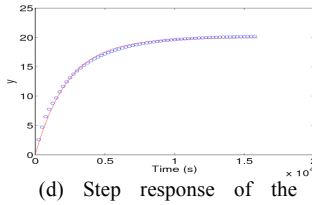

(d) Step response of the system and transfer function u_2-y_2)

Fig. 6. Step response of the system (symbol "o") and the identified transfer functions (Continuous curves)

7 QDMC Control of FCC

7.1 Generality

The FCC control will be carried out with several cases: First, the control will use two manipulated and two controlled variables, then three manipulated and two controlled variables.

7.2 QDMC 2X2 control

In the present case, constraints are imposed on the manipulated variables (Table 5). The set points are known a priori. Set points are chosen in a desynchronized manner so as to better show the input-output coupling effect within the process. Two cases have been studied (Table 5). The simulations results (Figures 7 (c), 7 (d), 7 (a), 7 (b) show that despite the changes in the set point, the outputs follow the set point with deviation respectively of 1 to 2K at most whereas the manipulated variable remain within the constraints limits. The results (Figures 8 (c), 8 (d), 8 (a), 8 (b)) show the controller performance in the case of reduced weights on the outputs. The manipulated variables remain in the limits of constraints and the outputs continue to follow their respective set points in an acceptable manner.

Table 5. MPC parameters 2X2

Parameters	Case 1	Case 2
Sampling period	250s	250s
Prediction horizon	60	20
Control horizon	3	3
Constraints Min-Max on the input 1	[270, 320]	[270, 320]
Constraints Min-Max on the input 2	[24, 50]	[24, 50]
Γ diagonal values	10 10	3 3
Λ diagonal values	1 1	10 1 0

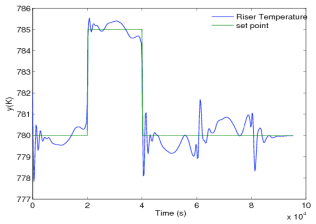

(a) Temperature at the riser top y_1 (K)

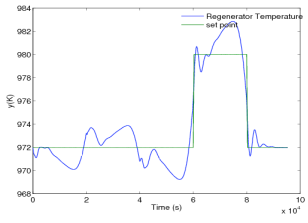

(b) Temperature in the regenerator y_2 (K)

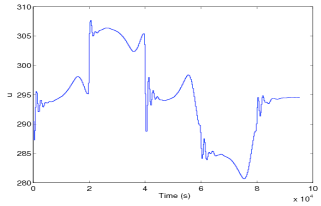

(c) Flow rate of regenerated catalyst u_1 (kg.s^{-1})

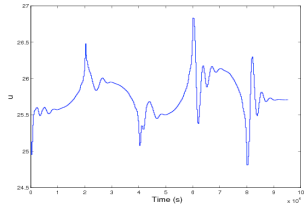

(d) Flow rate of air to the regenerator u_2 (kg.s^{-1})

Fig. 7. QDMC control 2X2, case 1: Controlled and manipulated variables

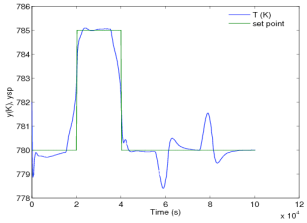

(a) Temperature at the riser top y_1 (K)

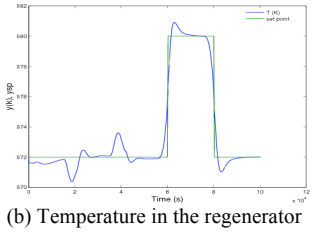

(b) Temperature in the regenerator y_2 (K)

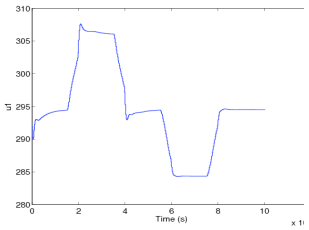

(c) Flow rate of regenerated catalyst u_1 (kg.s^{-1})

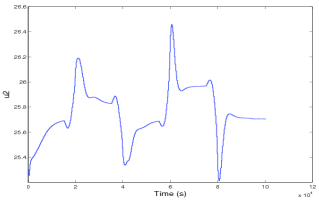

(d) Flow rate of air to the regenerator u_2 (kg.s^{-1})

Fig. 8. QDMC 2X2, case 2: Controlled and manipulated variables

The coupling effects are visible on Figures 7(c), 7(b), 7(d), 7(a). For example, output 1 returns quickly to its steady state after a transient while output 2 follows its new set point. Hence, QDMC based on step responses is able to maintain the outputs of a complex process near its variable set points with acceptable deviations.

The influence of the weights on the criterion has been studied (Table 5). The energy part is given less weight than the performance one . This led to correct tracking (Figures 7(a), 7(b)) but, at the same time we notice some steep variations changes of the inputs, visible at set point changes. The reduction of the weights Γ (Figures 8 (a) and 8 (b)) leads to less acceptable tracking of the set point with important temperature deviations around the set point changes, but this remains acceptable. The inputs in this case are more smooth.

Some variables such as the coke concentrations on the catalyst in the separator and in the regenerator, the molar fraction of oxygen in the regenerator dense bed are presented in Figures 9, 10. Figure 9 shows that the coke on the catalyst is not completely burnt which agree with the hypothesis that the regenerator is in partial combustion mode. The coke content at the riser top is similar to the coke in the separator and follows the same evolution as the coke in the regenerator, so when the regenerator temperature increases, the coke content decreases also and when the temperature in the riser increases, the coke content increases also. The increase of the air flow rate in the regenerator leads to the decrease of the quantity of coke in the regenerator as well as in the separator. The variations of the molar fraction of oxygen in the regenerator (Figure 10) are in the opposite way to the variations of the the coke in the regenerator, so when the coke is high, the oxygen molar fraction is low and this is due to the fact that oxygen is consumed in a great quantity and reciprocally.

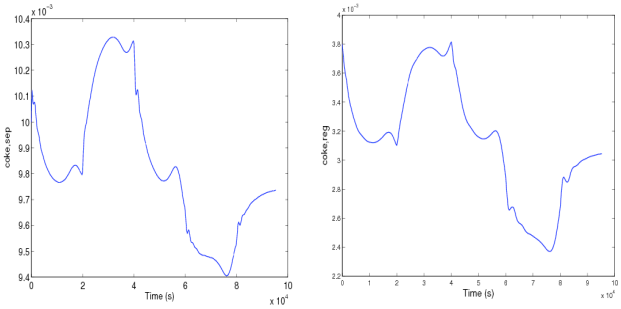

Fig. 9. QDMC 2X2, case 1: Mass fraction of coke on the catalyst in the regenerator (left), Mass fraction of coke on the catalyst in the separator (right)

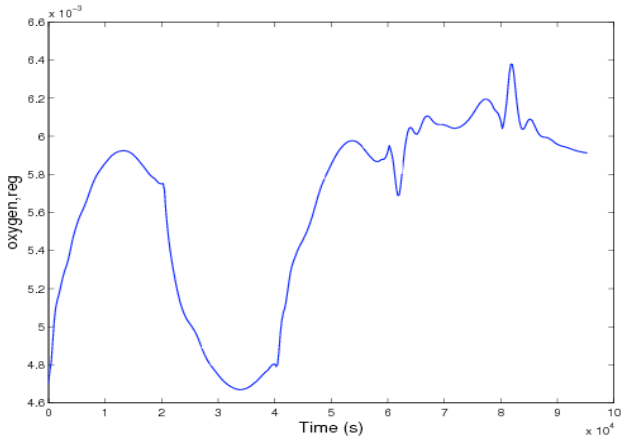

Fig. 10. QDMC 2X2, case 1: Molar fraction of oxygen in the regenerator

7.2.1 Disturbance rejection

Many possible disturbances exist, in particular the feed flow rate, the quality of feed, the temperature of the feed, the temperature of air entering the regenerator, the hold up of catalyst in the regenerator.

In the present case, a series of disturbances of the feed flow rate is introduced by 5 % increase of the feed flow rate at $t = 25000$ s, then a decrease by 10% at t=50000s and again back to it initial level at t=75000s. Figures 10, 10, 10, 10 present the results of simulations in the case of feed disturbance with constant set point. The disturbances are well rejected by QDMC control. The temperature at the riser top varies in opposite direction with regard to the feed flow rate and dispalys a peak of about 5K for a variation of 5% of the feed flow rate. The temperature in the regenerator varies in a more complex manner with first a fast deviation of about 2K in the inverse direction of the variation of 5% of the feed flow rate, followed by a slower deviation of about 2K in the direction of the variation of the feed flow rate. Thus, it takes more time for the regenerator temperature to come back to its set point than the riser top temperature. The control u_1, corresponding to the flow rate of regenerated catalyst, increases of about 5% when the feed flow rate increases and the control u_2, corresponding to the flow rate of air in the regenerator increases almost in the same proportion.

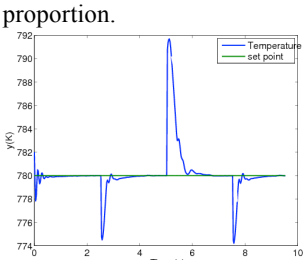

(a) Temperature at the riser top y_1 (K)

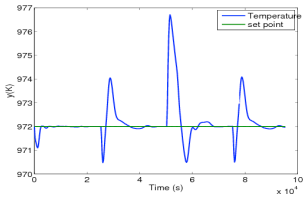

(b) Temperature in the regenerator y_2 (K)

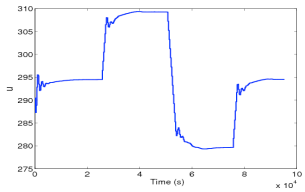

(c) Flow rate of regenerated catalyst u_1 (kg.s^{-1})

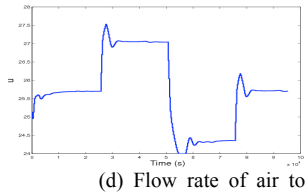

(d) Flow rate of air to the regenerator u_2 (kg.s^{-1})

Fig. 11. QDMC 2X2: Controlled and manipulated variables in the case

of feed flow rate disturbance (increase of 5% at t=25000s, decrease of 10% à t=50000s, then back to initial value at t=75000s)

7.3 QDMC 3X2 control

The QDMC 3X2 control has been studied by adding the feed flow rate as a manipulated variable (Table 6).

Table 6. Manipulated and controlled variables

3X2 control		
Input 1	Regenerated catalyst	u_1
Input 2	Flow rate of air to the regenerator	u_2
Input 3	Flow rate of feed	u_3
Output 1	Temperature at the riser top	y_1
Output 2	Temperature at the regenerator dense bed	y_2

Figures 12(a), 12(b) and 12(c) present the step responses for the identification of the FCC with three manipulated variables, the flow rate of regenerated catalyst, the flow rate of air to the regenerator and the feed flow rate. Simulations are carried out with the same tuning parameters as in the case of two manipulated variables (Table 5). Concerning the responses 5, the influence of the regenerated catalyst flow rate and the air flow rate are identical, whereas the influence of the feed flow rate show a response that is similar to a first order with a negative gain, this means that an increase of feed flow rate leads to a decrease of the temperature at the riser top and in the regenerator dense bed.

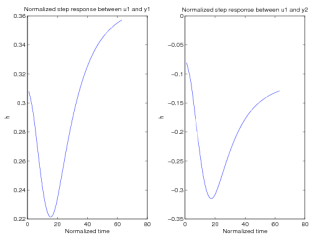

(a) Step response coefficients, influence of catalyst flow rate

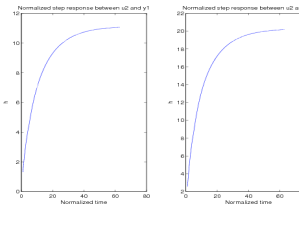

(b) Step response coefficients, influence of air flow rate

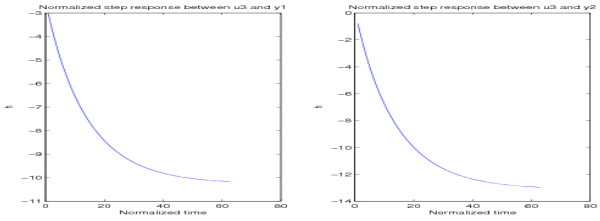

(c) Step response coefficients, influence of feed flow rate

Fig. 12. Step response coefficients for QDMC 3X2 control: u_1 flow rate of regenerated catalyst , u_2 flow rate of air, u_3 feed flow rate, y_1 riser temperature, y_2 regenerator temperature

Table 7. MPC parameters 3X2

Paramètres	Values
Sampling period	250s
Prediction horizon	60
Control horizon	3
Contrainst Min-Max input 1	[270, 320]
Contrainst Min-Max input 2	[24, 50]
Contrainst Min-Max input 3	[15, 70]
Γ diagonal value	5 10
Λ diagonal value	1 1 1

QDMC 3X2 has been carried out with the tuning of Table 7. Figure 13 represents the temperature at the riser top and in the regenerator dense bed, Figure 14 the manipulated variables during the control. The set point are well tracked with oscillations around the set point changes .

In fact, it is interesting to compare the results of the QDMC 3X2 control (Figures 13 and 14) to the results of QDMC 2X2 control (Figure 7). The set point tracking is improved for QDMC 3X2 control, but at the expense of oscillations of the temperature at the riser top which are not desirable and are tied to oscillations of the inputs.

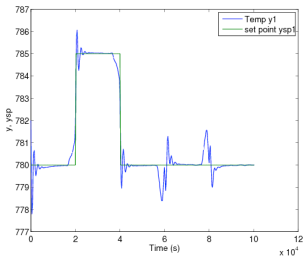

(a)Temperature at the riser top (K)

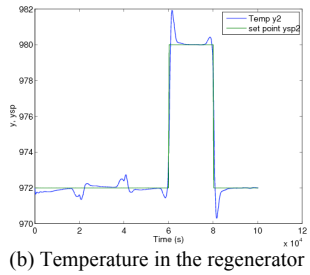

(b) Temperature in the regenerator (K)

Fig.13. 3X2 control: controlled variables

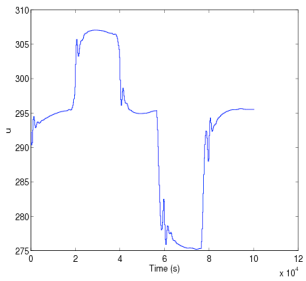

(a) Flow rate of regenerated catalyst ($kg.s^{-1}$)

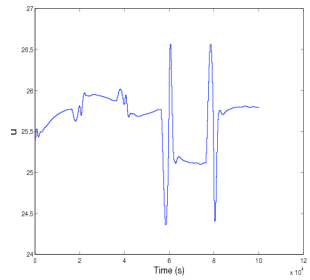

(b) Flow rate of air to the regenerator ($kg.s^{-1}$)

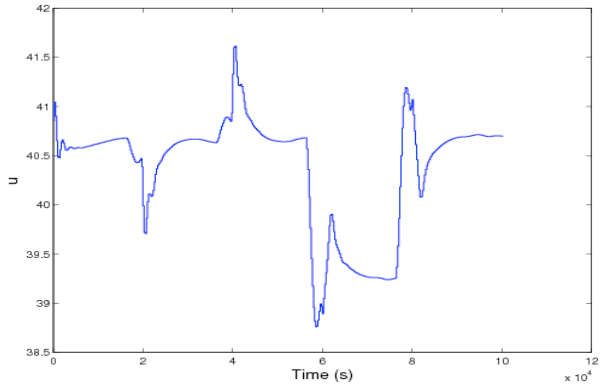

(c) Feed flow rate ($kg.s^{-1}$)

Fig. 14. QDMC 3X2 control : Manipulated variables

8 MPC tuning

The results of simulation presented up to now have been obtained with the same MPC parameters. However, the tuning of FCC control is of critical importance in order to obtain good behavior. In this part, the influence of MPC parameters on the simulation results will be presented and

tuning solutions proposed for these parameters with respect to the QDMC algorithm applied to the FCC. Table 8 presents the different cases of parameters used in the simulations.

Table 8. MPC tuning parameters

	T	Horizon H_P	Horizon H_C	Contrainst Min-Max on input 1	Contrainst Min-Max on input 2	γ values diagonals	H
Case 1	*250 s*	*60*	*3*	*[270,320]*	*[24,50]*	*10 10*	*1 1*
Case 2	*250 s*	*20*	*3*	*[270,320]*	*[24,50]*	*10 10*	*1 1*
Case 3	*250 s*	*60*	*3*	*[270,320]*	*[24,50]*	*2 2*	*1 1*
Case 4	*250 s*	*60*	*3*	*[270,320]*	*[24,50]*	*2 2*	*15 15*
Case 5	*250 s*	*20*	*3*	*[270,320]*	*[24,50]*	*10 10*	*15 15*
Case 6	*250 s*	*20*	*3*	*[270,320]*	*[24,50]*	*2 2*	*15 15*
Case 7	*250 s*	*60*	*3*	*[270,320]*	*[24,50]*	*5 5*	*1 1*

The notations of table 8 are the sampling period T_s, the prediction horizon H_p, the control horizon H_c, the minimal value of the prediction instant $H_{p,low}$.

Case 1 (Figures 15 and 16) can be considered as a basic case for the tuning parameters and all the following comparisons are done with respect to case 1 or derived cases. Table 8 can be considered as a numerical experimental design . However, the tuning of case 1 cannot be consider to be optimal because it would have been needed to define an optimality criterion such as a statistical criterion based on deviations or simply the value of the quadratic criterion considering $H_{p,low} = 1$ in all the cases . In case 2 (Figures 17 and 18), the prediction horizon is decreased, this decreases the oscillations when the set point constraints are imposed. The manipulated variables vary more smoothly.

In case 3 (Figures 19 and 20), the weight on the outputs is decreased to give more weight to the energy part of the criterion with regard to the performance. Smooth responses are expected due to smoother manipulated inputs, which really occurs, however the temperature tracking is less satisfactory.

In case 4 (Figures 21 and 22) compared to case 3 the minimal horizon $H_{p,low} = 15$ is used. The control is very smooth, but the set point tracking is not satisfactory.

In case 5 (Figures 23 and 24), the prediction horizon is decreased as $H_p = 15$ with $H_{p,low} = 10$. As the weights on the outputs remain high, the responses are satisfactory and smooth with an anticipating effect of the set point changes.

In case 6 (Figures 25 and 26), compared to the previous case, more weight is given to the energy term of the criterion, and the inputs are softened with respect to to case 5, however the difference is small.

In case 7 (Figures 27 and 28), instead of brutal set point steps, a reference trajectory is imposed as a linear ramp over 12 sampling periods. The consequence is that the oscillations visible in the case 1 at the set point changes are almost eliminated and the tracking of set point is excellent.

A conclusion of all the tuning is that the filtering of the set point brings more smoothness in this case of difficult control, for the steps of flow rate of catalyst create strong inverse response added to an important algebraic effect. It is important to use large weights on the outputs. The use of the lower limit of the prediction horizon $H_{p,low}$ did not have the expected effect.

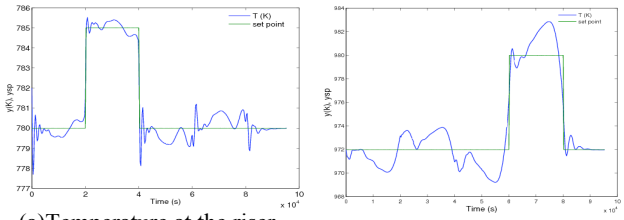

(a)Temperature at the riser top (K) (b)Temperature in the regenerator (K)

Fig. 15. QDMC control, case 1: Controlled variables

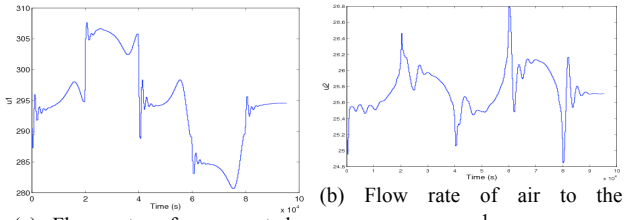

(a) Flow rate of regenerated catalyst (kg.s $^{-1}$) (b) Flow rate of air to the regenerator (kg.s $^{-1}$)

Fig. 16. QDMC control, case 1: Manipulated variables

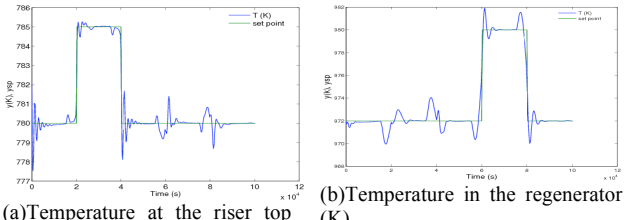

(a)Temperature at the riser top (K) (b)Temperature in the regenerator (K)

Fig. 17. QDMC control, case 2: Controlled variables

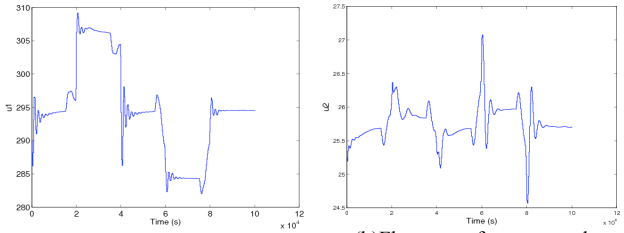

(a) Flow rate of regenerated catalyst (kg.s $^{-1}$) (b)Flow rate of regenerated catalyst (kg.s $^{-1}$)

Fig. 18. QDMC control, case 2: Manipulated variables

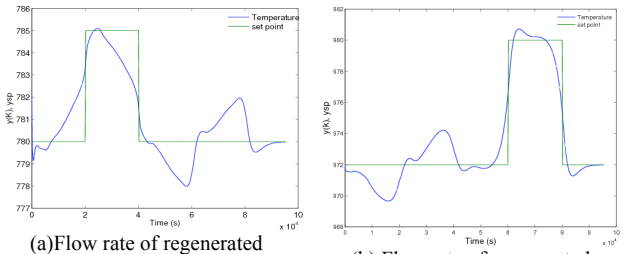

(a)Flow rate of regenerated catalyst (kg.s $^{-1}$) (b) Flow rate of regenerated catalyst (kg.s $^{-1}$)

Fig. 19. QDMC control, case 3: Controlled variables

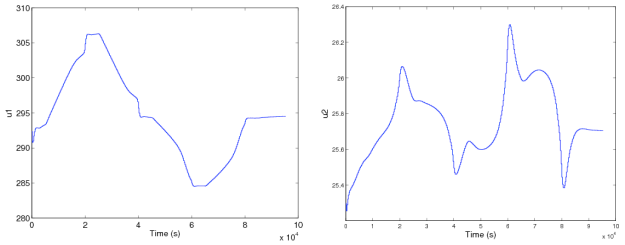

(a)Flow rate of regenerated catalyst (kg.s $^{-1}$) (b) Flow rate of air to the regenerator(kg.s $^{-1}$)

Fig. 20. QDMC control, case 3: Manipulated variables

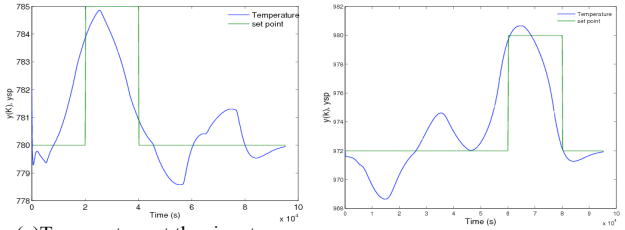

(a)Temperature at the riser top (K) (b)Temperature in the regenerator (K)

Fig. 21. QDMC control, case 4: Controlled variables

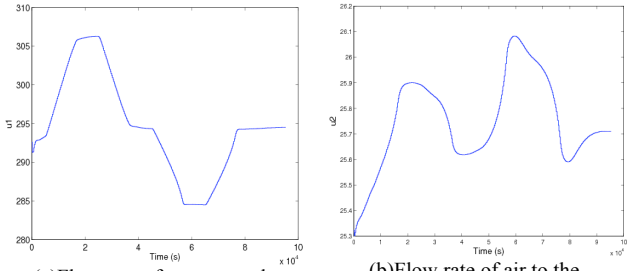

(a)Flow rate of regenerated catalyst (kg.s $^{-1}$) (b)Flow rate of air to the regenerator (kg.s $^{-1}$)

Fig. 22. QDMC control, case 4: Manipulated variables

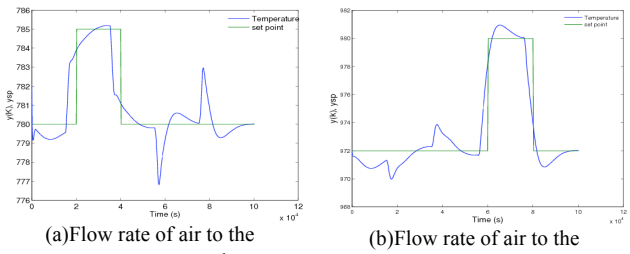

(a)Flow rate of air to the regenerator (kg.s $^{-1}$) (b)Flow rate of air to the regenerator (kg.s $^{-1}$)

Fig. 23. QDMC control, case 5: Controlled variables

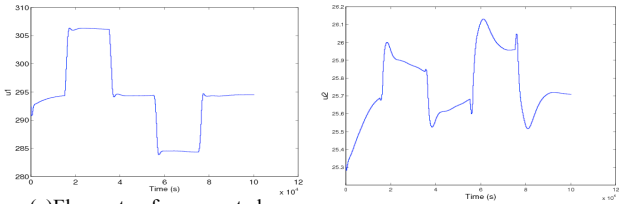

(a)Flow rate of regenerated catalyst (kg.s $^{-1}$) (b)Flow rate of air to the regenerator(kg.s $^{-1}$)

Fig. 24. QDMC control, case 5: Manipulated variables

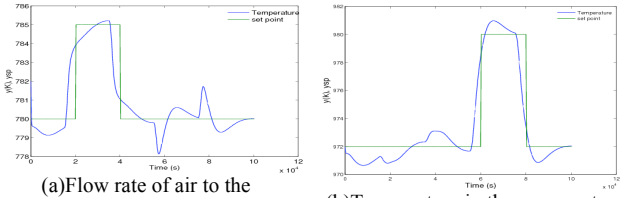

(a)Flow rate of air to the regenerator(kg.s $^{-1}$) (b)Temperature in the regenerator (K)

Fig. 25. QDMC control, case 6: Controlled variables

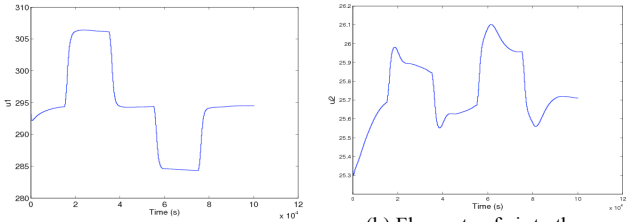

(a) Flow rate of regenerated catalyst (kg.s $^{-1}$) (b) Flow rate of air to the regenerator(kg.s $^{-1}$)

Fig. 26. QDMC control, case 6: Manipulated variables

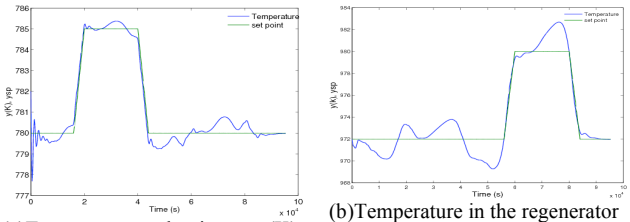

(a)Temperature at the riser top (K) (b)Temperature in the regenerator (K)

Fig 27. QDMC control, case 7: Controlled variables

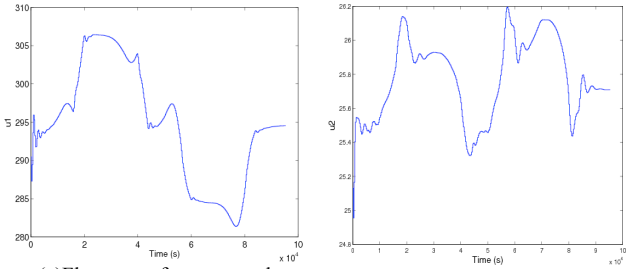

(a)Flow rate of regenerated catalyst (kg.s $^{-1}$) (b)Flow rate of regenerated catalyst (kg.s $^{-1}$)

Fig. 28. QDMC control, case 7: Manipulated variables

9 FCC parameters estimation

Many parameters of the FCC are difficult to measure. The coke content of catalyst at the regenerator exit and the coke content on the catalyst at the riser top are among the main parameters. Other parameters although measurable, must be estimated to allow a monitoring of the process and to continue to control the process even when some sensors are faulty. This includes for example the temperature in the

differents bed of the regenerator and the temperature in the riser.

The estimation technique used is based on the extended Kalman filter to which the MPC control system of the FCC is coupled. This enables us to have an estimation of some parameters while controlling on line the system. The estimation is used here for monitoring purpose. The estimated variables are not used by the predictive control part.

9.1 Estimation of state parameters principles

The EKF is an extension of the linear Kalman filter in the case of a non linear system. The nonlinear model is linearized in the prediction phase, then a correction using the Kalman gain and measurements is performed in order to obtain the state estimations [14].

In the present case, the continuous-discrete EKF is used as in most industrial cases [21]. It is based on a continuous time model and discrete measurements.

The state equation is represented by

$$\dot{x}(t) = f(x,u,\theta,t) + w \quad (16)$$

w is a Gaussian noise of zero mean with covariance matrix Q. At time k, the output equation is represented by

$$z_k = h(x_k) + v_k \quad (17)$$

where v_k is a discrete Gaussian white noise of zero mean and covariance matrix R_k.

The states at time k are estimated using measurements at time k. The algorithm is decomposed in a first phase of prediction, followed by correction:

1 Propagation of the state estimation and the error covariance:

the continuous differential equations describing the variation of the state vector x and of the error covariance matrix P are integrated on the time interval $[k-1,k]$ to obtain the predictions respectively noted $x_k(-)$ and $P_k(-)$. z_k are the measurements.

2 Update of the state estimation and the error covariance:

At each sampling instant t_k, the state estimation and the covariance are updated as

$$\begin{aligned} \hat{x}(+) &= \hat{x}_k(-) + K_k[z_k - h(\hat{x}_k(-))] \\ P_k(+) &= [I - K_k H_k(\hat{x}_k(-))]P_k(-) \end{aligned} \quad (18)$$

where K_k is the Kalman gain matrix given by

$$K_k = P_k(-)H_k^T(\hat{x}_k(-))[H_k(\hat{x}_k(-))P_k(-)H_k^T(\hat{x}(-)) + R_k]^{-1} \quad (19)$$

and H_k is the jacobian h given by

$$H_k(\hat{x}_k(-)) = \left(\frac{\partial h}{\partial x}\right)_{x=\hat{x}_k(-)} \quad (20)$$

The corrected estimations are $\hat{x}(+)$ and $P_k(+)$.

9.2 Results and discussion

The tuning of the Kalman filter is done with the values in Table 9.

∫ Tuning parameters of Kalman filter

Parameters	Values
Number of measured outputs	2
Number of estimated states	5
standart deviation measurement noise de mesure	$\sigma = 0.3$
Covariance matrix Q	diagonal 10^{-3}
Covariance matrix R	diagonal σ^2
Initial values of estimated states	
Mass fraction of coke in the separator	0.01
Separator temperature (K)	780
Mass fraction of coke in the regenerator	0.0032
Regenerator temperature (K)	970
Molar fraction of O_2 in the regenerator	0.004

Figures 30 (a), 30 (b), 29 (a), 29 (b) present the estimated parameters such as mass fraction of coke on the catalyst in the regenerator, mass fraction of coke on the catalyst in the separator and measure and estimated temperature in the regenerator molar fraction of oxygen in the regenerator. When we examin these results, we see that extended Kalman filter gives a good estimate of all these parameters.

A study of the robustness of the estimator have been carried out. For this reason, the model used for the estimation has been chosen volontarily different from the process model consider as perfect. The difference in the model concern some constant for which we have chosen differents values. So, the hold up of solid in the regenerator is decrease of 0.1 %.

Figures 29 (c) present the measured temperature and the estimated temperature with the estimator model different from the real process model. We notice that the estimation gives reliable results even in the case of erronoeus model use by Kalman filter., this is normal because the temperature is measured and the estimator just filters the measures. Figure 30 (c) presents mass fraction of coke in the regenerator in the case of the estimator model different to the process model. We notice an estimation which present a great deviation which increases with time. This is tied to the influence of the model errors on certains estimations. In fact, the decrease of the hold up of catalyst in the regenerator of 0.1 % is enough to increase the mass fraction of coke produced; this is justified when we look at the differential equation which describe the mass fraction of coke in the regenerator. We have to notice that an important modification of the model does not permit a reliable estimation for, the reduced system use by Kalman filter can become unstable. In fact, the problem is tied to the instability of the process due to the recycle coke as soon as we go too much beyong it nominal state. Figure 30 (d) present the estimation of the mass fraction of coke in the regenerator, the real coke in the regenerator, the coke with

the modified model of the estimator and the coke at the riser top. We notice that the regenerator is run on partial combustion mode for the coke is not completly burn in the regenerator.We also notice that the coke in the regenerator has the same appearance as the coke at the riser top, the only different being the different amplitude level which is due to coke combustion in the regenerator.

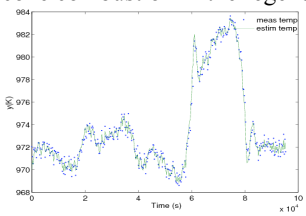

(a) Measured and estimated temperature in the regenerator

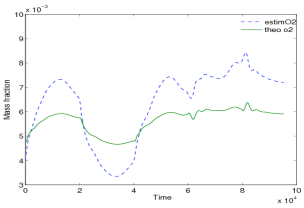

(b) Molar fraction estimated and theoritical in the regenerator

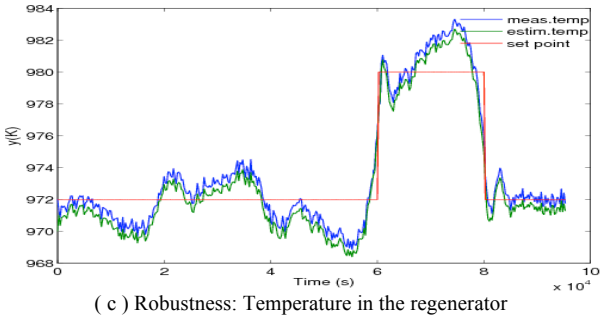

(c) Robustness: Temperature in the regenerator

Fig. 29. Temperature, molar fraction

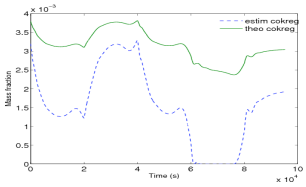

(a) Estimated and theoritical coke in the regenerator

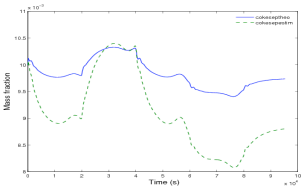

(b)Estimated and theoritical coke in the separator

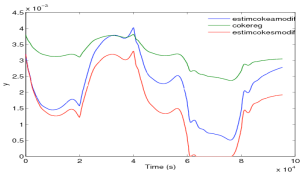

(c) Estimation of coke in the regenerator with modified model and real coke

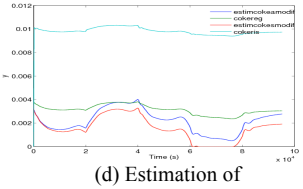

(d) Estimation of regenerator coke with modified model, real coke, coke at the top of the riser

Fig. 30. theoritical, estimated, modified model parameters

10 Conclusion

In this work, model predictive control algorithm was used along with the extended Kalman filter for online state estimation and control of the FCC unit . The manipulated variable used were the regenerated catalyst flow rate , the flow rate of air to the regenerator and the flow rate of feed to the riser . A novel four transfer functions were identified and proposed. Two control structures were studied, 2X2 and 3X2. Simulation results showed a very good tracking of the set points of the top or riser and regenerator temperatures and feed disturbances were well rejected. As these temperatures were successfully followed despite the strong interactions between the riser and the regenerator, the yield of products such as gasoline and, more generally, the overall yield of an FCC unit can be improved while taking into account the different constraints of the process. MPC tuning was studied and showed that the filtering of the set point brings more smoothness and that it is important to use large weights on the outputs to achieve good tracking. Online state estimation is carried out. Results show estimation that are reliable even when model mismatch is tested.

References

1. J. Alvarez-Ramirez, J. Valencia, and H. Puebla. Multivariable control configuration for composition regulation in a fluid catalytic cracking unit. *Chem. Eng. J.*, 99:187–201, 2004.
2. A. Arbel, I.H. Rinard, and R. Shinnar. Dynamic and control of fluidized catalytic crackers. 3. Designing the control system: choice of manipulated and measured variables for partial control. *Ind. Eng. Chem. Res.*, 35:2215–2233, 1996.
3. J.S. Balchen, D. Ljungquist, and S. Strand. State-space predictive control. *Chem. Eng. Sci.*, 47(4):787–807, 1992.
4. A. T. Boum, A. Latifi, and J. P. Corriou. Model predictive control of a fluid catalytic cracking unit. In *2013 International Conference on Process Control (PC)*, pages 335–340, Strbské Pleso, Slovakia, 2013.
5. A. T. Boum, A. Latifi, and J. P. Corriou. Model predictive control of a fluid catalytic cracking process. In *Récents Progrès en Génie des Procédés*, Ed. SFGP, Paris, France, 2013.
6. E.H. Bristol. On a new measure of interactions for multivariable process control. *IEEE Trans. Automat. Control*, AC-11:133–134, 1966.
7. E. F. Camacho and C. Bordons. *Model predictive control*, volume 2. Springer London, 2004.
8. J. P. Corriou. *Commande des Procédés*. Lavoisier, Tec. & Doc., Paris, third edition, 2012.
9. C.R. Cutler and B.L. Ramaker. Dynamic matrix control-a computer control algorithm. Houston,Texas, 1979. In AIChE Annual Meeting.
10. J.B. Froisy. Model predictive control: past, present and future. *ISA Transactions*, 33:235–243, 1994.
11. C.E. Garcia and A.M. Morshedi. Quadratic programming solution of dynamic matrix control(qdmc). *Chem.Eng Comm*, 46:73–87, 1986.
12. C.E. Garcia, D.M. Prett, and M. Morari. Model predictive control: Theory and practice - a survey. *Automatica*, 25(3):335–348, 1989.
13. C.E. Garcia. Quadratic dynamic matrix control of nonlinear processes - an application to a batch reaction process. In *AIChE Annual Meeting*, San Franciso, USA, 1984.
14. E.L. Haseltine and J.B. Rawlings. Critical evaluation of the extended Kalman filtering and moving-horizon estimation. *Ind. Eng. Chem. Res.*, 44:2451–2460, 2005.
15. M. Hovd and S. Skogestad. Controllability analysis for the fluid catalytic cracking process. *AIChE Annual Meeting*, 1991.
16. M. Hovd and S. Skogestad. Procedure for regulatory control structure selection with application to the FCC process. *AIChE J.*, 39(12):1938–1953, 1993.
17. E. Lee and F.R.Jr. Groves. Mathematical model of the fluidized bed catalytic cracking plant. *Trans. Soc. Comput. Sim.*, 2:219–236, 1985.
18. G. Pandimadevi, P. Indumathi, and V. Selvakumar. Design of controllers for a fluidized catalytic cracking process. *Chem. Engng. Res. D.*, 88(7):875–880, 2010.
19. C. I. C. Pinheiro, J. L. Fernandes, L. Domingues, A. J. S. Chambel, I. Graça, N. M. C. Oliveira, H. S. Cerqueira, and F. R. Ribeiro. Fluid catalytic cracking (fcc) process modeling, simulation, and control. *Ind. Eng. Chem. Res.*, 51:1–29, 2011.
20. J. Richalet, A. Rault, J.L Testud, and J. Papon. Model predictive heuristic control: Applications to industrial processes. *Automatica*, 14:413–428, 1978.
21. D. Simon. *Optimal State Estimation - Kalman, H_∞ and Nonlinear Approaches*. Wiley, Hoboken, New Jersey, 2006.